Supporting Information
Predicting Au-S bonds breakage from the swelling behavior of surface tethered polyelectrolyte

Yanxia Zhang,[a,b,c] Bei'er lv,[b] Zhongyuan Lu,[d] Jian'an He,[b] Shen Zhang,[b] Hong Chen*[a] *and* Hongwei Ma*[b]

[a] College of Chemistry, Chemical Engineering and Materials Science, Soochow University, Suzhou, 215123, P. R. China; [b] Division of Nanobiomedicine, Suzhou Institute of Nano-Tech and Nano-Bionics, Chinese Academy of Sciences, Suzhou, 215123, P. R. China; [c] School of materials science and engineering, Wuhan University of technology, Wuhan, 430070, P. R. China; [d] State Key Laboratory of Theoretical and Computational Chemistry, Institute of Theoretical Chemistry, Jilin University, Changchun, 130023, P. R. China.

Well controlled preparation of samples

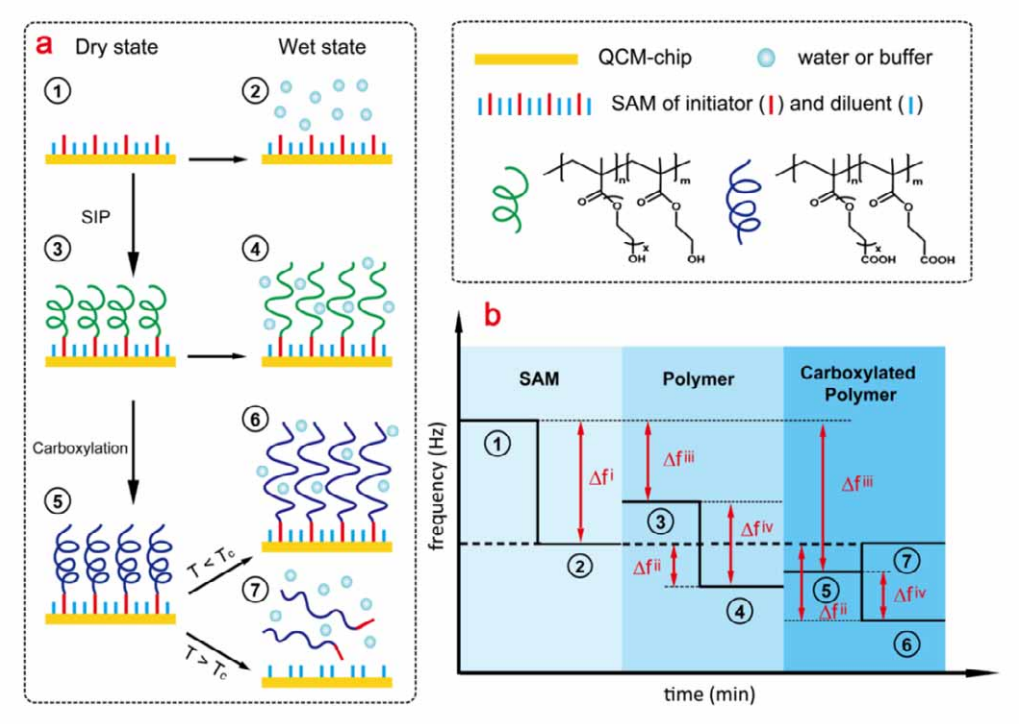

Scheme S1 Illustration of the experimental design. (a) Status of quartz chip: an initiator SAM functionalized quartz chip vibrating in air (dry state ①) and in water or buffer (wet state ②), poly(OEGMA-r-HEMA) coated chip in air (state ③) and in water (state ④), carboxylated poly(OEGMA-r-HEMA) coated chip in air (state ⑤) and in water/PBS (state ⑥ or ⑦). Each state in the surface modification has its corresponding frequency measurement as indicated in (b). Note that the molecular structure of carboxylated polymers was simplified.

Scheme S1 described the experimental design: a bare QCM chip was first measured for its absolute frequency at air, which was set to be the zero reference point. All the frequency changes due to surface modifications or swelling were referenced to this zero point. There was no measurable frequency difference for QCM chips with and without self-assembled monolayer (SAM) modification.[1] Thus, for convenience, initiator SAM modified QCM chip (state ①) was also

referenced as the zero point. The QCM chip was then exposed to liquid (state ②), which led to the first measured frequency change, termed as Δf^{i} for historical reason[1]. For Milli-Q water and PBS, Δf^{i} = -400 Hz (all experiments were conducted at 25°C unless otherwise stated).

After surface initiated polymerization (SIP) as well as carboxylation, the polymer coated QCM chips (state ③ and ⑤, respectively) were measured at air (Δf^{iii}). The thickness of the film was controlled via varying SIP time. Ellipsometry results revealed a linear equation between the dry thickness of polymer layer before ($T_{OH,\,dry}$) and after ($T_{COOH,\,dry}$) carboxylation (Fig. S1). The linear relationship between $T_{COOH,\,dry}$ and $T_{OH,\,dry}$ suggested that the permeability of the films to small molecules, e.g., succinic anhydride, was independent of the film thickness.

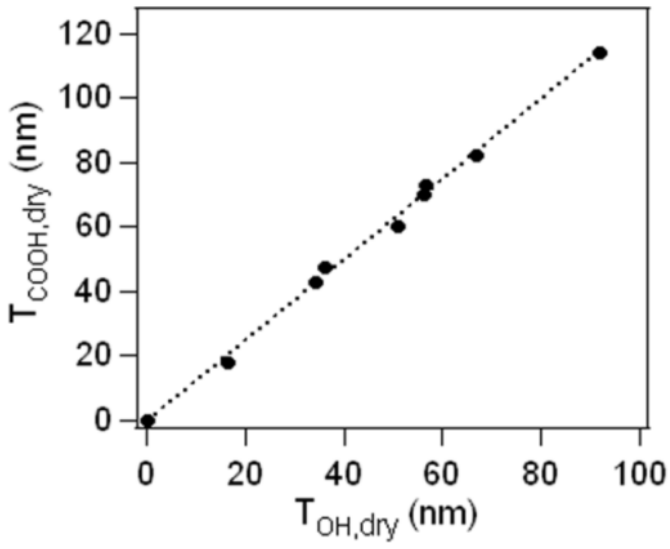

Fig. S1 Linear relations between thickness of polymer before ($T_{OH,\,dry}$) and after ($T_{COOH,\,dry}$) carboxylation: $T_{COOH,\,dry} = k' T_{OH,\,dry}$, where k' = 1.22. The R^2 values for linear fits were > 0.995.

To summarize, the ability to control thickness via SIP enabled us to prepare probes (i.e., polymer coating on QCM chips) in a custom-tailored fashion. Probes with $T_{COOH,\,dry}$ from 20 nm to 120 nm were obtained. For all these polymers, we had $\Delta f^{iii} = k_{2,dry} T_{dry}$, where T_{dry} is the thickness of

polymer layer in the dry state, and $k_{2,dry}$ is the slope (Fig. S2). Such linear relation was in agreement with our previous reports[1,2] and was used as a check-point for sample quality control.

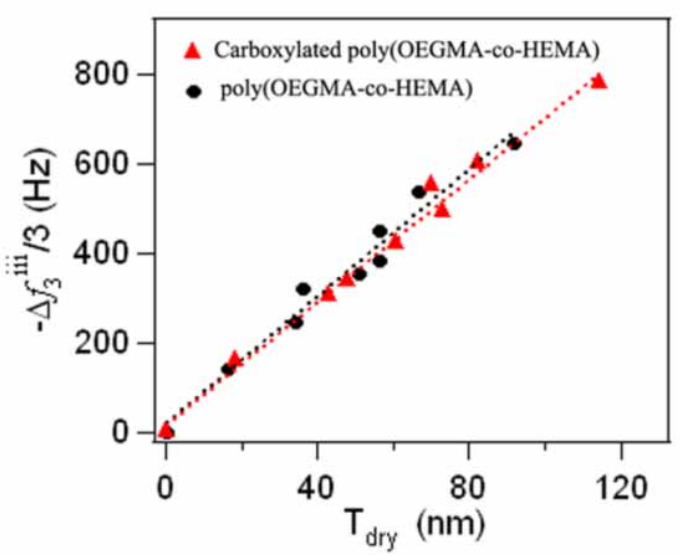

Fig. S2 Linear relations between frequency changes (Δf^{iii}) and thickness (T_{dry}): $\Delta f^{iii} = -k_{2,dry}T_{dry}$, where $k_{2,dry}$ is 7.57 and 7.12 for poly(OEGMA-r-HEMA) and carboxylated poly(OEGMA-r-HEMA), respectively. The R^2 values for linear fits were > 0.95.

The polymer coated QCM chips were then measured at water or PBS (state ④ and ⑥, $\Delta f^{iii} + \Delta f^{iv}$). Note that Δf^{iii} was determined from a discontinuous mode, while Δf^{i} and $\Delta f^{iii} + \Delta f^{iv}$ were determined from a continuous mode (i.e., no QCM chip reloading step). From previous studies, we had $\Delta f^{ii} = \Delta f^{iii} + \Delta f^{iv} - \Delta f^{i}$. The Δf^{ii} was induced by the mass of deposited polymer (i.e., the dry mass), entrapped water and viscoelastic damping, which were collectively sensed by QCM as the wet mass.[3] A similar linear relation between $\Delta f_3^{ii}/3$ and T_{dry} was identified for polymer and expressed as $-\Delta f_3^{ii}/3 = k_{1,3}T_{dry,}$ where $k_{1,3}$ = 20.8 and 9.9 for neutral and carboxylated polymer in water, respectively. However, the linear relation working range was limited to 40 nm for neutral poly(OEGMA-r-HEMA), which was much smaller than the thickness of linear range for

carboxylated poly(OEGMA-r-HEMA) polymers (Fig. S3). The deviation from linear to nonlinear was attributed to the penetration depth (δ) of the thickness-shear wave of QCM:

$$\delta = \sqrt{\frac{2\eta}{\rho\omega}}$$

where ω is the angular excitation frequency, η and ρ are the viscosity and density of liquid over layer, respectively. δ describes how far the shear wave propagates into the surrounding medium (in this case the polymer film).[4] The larger the δ, the wider the linear range. Compared with the carboxylated polymers, the neutral ones showed the good solubility in water, and this highly extended chains had the lower viscosity and a lower δ value and finally a narrower linear range than the carboxylated films.

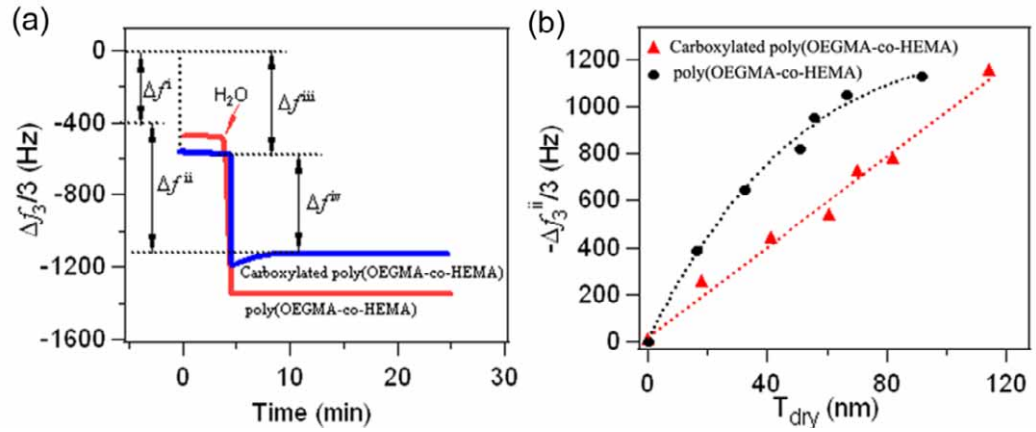

Fig. S3 The relations between frequency changes in water (Δf^{ii}) and dry thicknesses of polymer films (T_{dry}). (a) Applying Milli-Q water to poly(OEGMA-r-HEMA) before and after carboxylation ($T_{COOH,\ dry}$ = 70.1 nm). (b) The linear relations between Δf^{ii} and T_{dry} are wider for carboxylated polymer films than the neutral ones.

T_{eff} was calculated based on "solidified liquid layer" model

The focus of this study was the swelling behavior of the surface tethered carboxylated poly(OEGMA-r-HEMA) in PBS, which was monitored via QCM. Previously, we introduced a "solidified liquid layer" model that enabled QCM to be used as a molecular ruler.[5] In this model, one first applied the equation[3, 5]: $-\Delta f^{ii} = An+Bn^2$ to extract the wet mass induced frequency change A. A is free of viscoelastic damping contribution which is included in the B value, and n is the overtone number. Second, one could calculate the thickness of the swelled layer (T_{eff}): $T_{eff} = \Delta m/\rho = A*C/\rho$, where Δm is area averaged mass change; C is 17.7 ng cm^{-2} Hz for an AT-cut, 5 MHz crystal; the density of liquid overlayer (ρ) with initiator density at 2.5% was approximated as the density of PBS itself as previously reported.[5] So the two parameters, $-\Delta f^{ii}$ and T_{eff}, were equivalent in reflecting the state of polyelectrolyte swelling.

The degree of ionization of a single polymer chain (α_B) in PBS

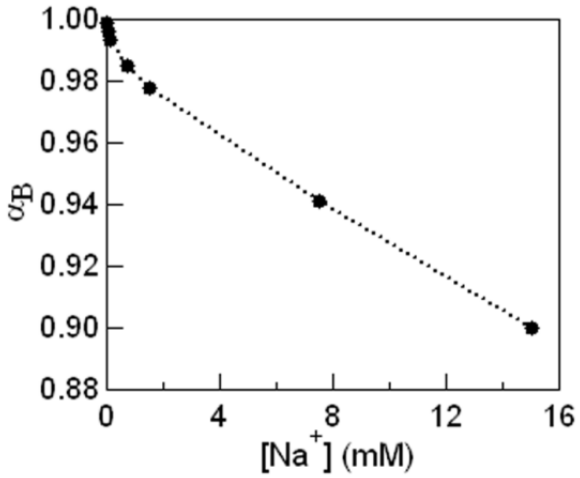

Fig. S4 The degree of ionization of a single polymer chain (α_B) in PBS (pH 7.4) was calculated by eq. (1) when using the experimental results of T_{eff}. α_B decreased with an increasing [Na^+].

The collapse of polyelectrolyte at high [Na^+]

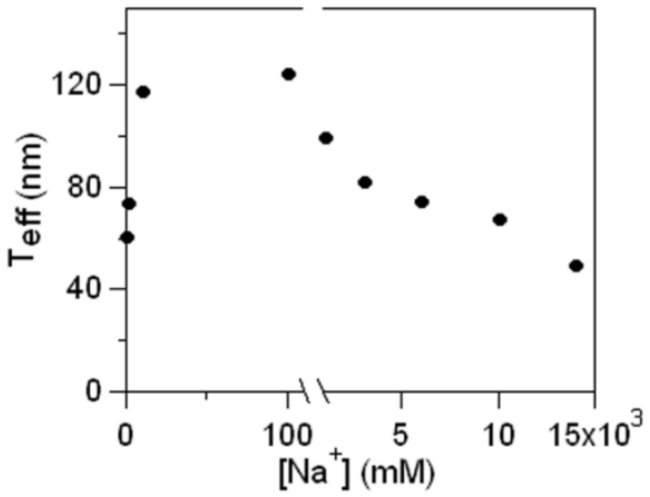

Fig. S5 Effect of [Na^+] on the swelling thickness (T_{eff}) of polyelectrolyte with $T_{COOH,\ dry}$ = 38.1 nm. Due to the good solubility in water, Na_2HPO_4 instead of NaCl was used in this study. It is found that T_{eff} increased with an increasing [Na^+] from 0.015 to 100 mM and a distinctive collapse was observed when [Na^+] > 1 M.

Computational Methods

In this study, all calculations were performed with density functional theory (DFT), as implemented in the Vienna *ab initio* simulation package (VASP)[6-8] with the projector-augmented wave method (PAW).[9-10] The energy was calculated using the generalized gradient approximation (GGA), non-self-consistently with RPBE functional.[11] Methfessel–Paxton[12] smearing with a width of 0.2 eV was used for efficiency. A 7 × 7 × 1 *k*-points grid was used to sample the Brillouin zone for surface calculations, with a 400 eV cutoff energy, which was found to be sufficient for energy and geometry convergence. All calculations were done at the non-spin-polarized level since spin polarization effects for each species were proved to be negligible. The metal surfaces (Pt (111), Au (111) and Ag (111)) were modeled using the repeated slab geometry, which was formed by

five-layer metal atoms. The slabs were separated by 15Å of vacuum, which guarantees no interaction between the slabs. Throughout our calculations, the adsorbed CH_3S molecules (where CH_3S could be considered as the representative headgroup of longer-chain alkanethiols) were only adsorbed on one side of the slab using the 2 × 2 surface models, corresponding to the coverage of 1/4 ML, and as usual, the two uppermost layers and adsorbate were allowed to fully relax whereas the innermost layers were fixed to bulk-like distances. For all calculations, geometry optimizations were stopped when all the forces (of the degrees of freedom set in the calculation) were smaller than 0.04 eV/Å.

The adsorption energies (ΔE_{ads}) were calculated based on the following equation:

$$\Delta E_{ads} = (E_{[slab]} + E_{[adsorbate]}) - E_{[slab + adsorbate]}$$

where $E_{[slab + adsorbate]}$, $E_{[slab]}$ and $E_{[adsorbate]}$ are the calculated electronic energies of adsorbed species on the metal surface, clean surface, and gas-phase molecule, respectively.

References

(1) Fu, L., Chen, X. N., He, J. A., Xiong, C. Y., Ma, H. W. *Langmuir* **2008**, *24*, 6100.

(2) He, J. A., Wu, Y. Z., Wu, J., Mao, X., Fu, L., Qian, T. C., Fang, J., Xiong, C. Y., Xie, J. L., Ma, H. W. *Macromolecules* **2007**, *40*, 3090.

(3) Zhang, Y. Z., Du, B. Y., Chen, X. N., Ma, H. W. *Anal. Chem.* **2009**, *81*, 642.

(4) Sharp, J. S., Forrest, J. A., Jones, R. A. L. Macromolecules **2001**, 34, 8752.

(5) Ma, H. W., He, J. A., Zhu, Z. Q., Lv, B. E., Li, D., Fan, C. H., Fang, J. *Chem. Commun.* **2010**, *46*, 949.

(6) Kresse, G., Hafner, J. *Phys. Rev. B* **1994**, *49*, 14251.

(7) Kresse, G., Furthmuller, J. *Comput. Mater. Sci.* **1996**, *6*, 15.

(8) Kresse, G., Furthmuller, J. *Phys. Rev. B* **1996**, *54*, 11169.

(9) Kresse, G., Joubert, D. *Phys. Rev. B***1999**, *59*, 1758.

(10) Blochl, P. E. *Phys. Rev. B* **1994**, *50*, 17953.

(11) Hammer, B., Hansen, L. B., Norskov, J. K. *Phys. Rev. B* **1999**, *59*, 7413.

(12) Methfessel, M., Paxton, A. T. *Phys. Rev. B* **1989**, *40*, 3616.